



# Physiochemical and thermal characterisation of faba bean starch

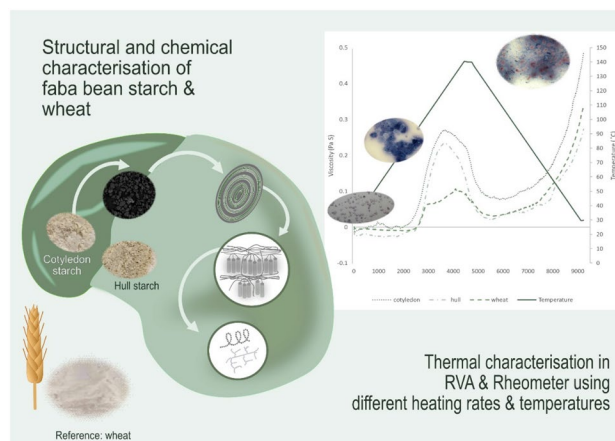
Klara Nilsson<sup>1</sup> · Corine Sandström<sup>1</sup> · Hüsamettin Deniz Özeren<sup>2,3</sup> · Francisco Vilaplana<sup>3</sup> · Mikael Hedenqvist<sup>2</sup> · Maud Langton<sup>1</sup>

Received: 26 April 2022 / Accepted: 14 July 2022 / Published online: 31 July 2022  
© The Author(s) 2022

## Abstract

The structure and physicochemical properties of starch isolated from the cotyledon and hull of faba beans and from wheat (as reference) were examined using 16 different methods. The amylose content in faba bean cotyledon and hull starch was 32% and 36%, respectively, and that in wheat starch was 21%. The faba bean cotyledon and hull starch were structurally alike both displaying C-polymorphic pattern, a similar degree of branching and similar branch chain length distributions. Wheat starch had a significantly greater prevalence of short amylopectin chains (DP < 12) and a higher degree of branching. Granules in both faba bean starches exhibited surface cracks and were more homogenous in size than the smoother wheat starch granules. Gelatinisation temperature was higher for the faba bean starches, likely as an effect of high amylose content and longer starch chains delaying granular swelling. Cotyledon starch produced pastes with the highest viscosities in all rheological measurements, probably owing to larger granules. Higher prevalence of lipids and resistant starch reduced the viscosity values for hull starch. For all starches, viscosity increased at faster heating rates. During the rheological analyses, the samples were exposed to different instruments, heating rates and temperatures ranges, differing from standard rheological procedures, which could help predict how different processing techniques effect the final starch textures.

## Graphical abstract



**Keywords** Amylose · Amylopectin · Degree of polymerisation · Gelatinisation · Rheology · High temperature pasting

## Introduction

The food sector accounts for approximately 30% of the world's total energy consumption and 22% of total greenhouse gas emissions [1]. To sustain the growing global

✉ Klara Nilsson  
klara.nilsson@slu.se

Extended author information available on the last page of the article

population while combating climate change, a shift towards plant-based dietary patterns is required [2, 3].

Wheat is Sweden's most cultivated crop and [4] has a relatively high soil nutrient requirement thereby increasing demand for mineral fertiliser. Correlation between years with high yields of wheat and sales of mineral fertilisers exists [5]. Negative environmental impact of mineral fertiliser are associated with nutrient leaching which can cause eutrophication and greenhouse gas emissions. In contrast faba beans (*Vicia faba* L.) a cool climate legume that is cultivated in several countries including Sweden [4], contributes to sustainable crop rotations because they can biologically fix atmospheric nitrogen (N<sub>2</sub>), thereby diversifying production systems [6]. In Sweden faba beans are currently primarily used as animal feed but the excellent nutritive qualities [7, 8] render them suitable for human consumption. Globally, faba bean is one of the leading crops used for producing pulse protein isolate [9], where starch represents a major side-stream component [3, 8]. To minimise the climate impact of faba bean production, all components of the beans should be utilised.

The physicochemical properties influencing food applications of starch are determined by chemical composition, molecular structure, crystallinity and granular morphology [10–12]. Starch, a glucose polymer, is composed of two types of polysaccharides, almost linear chain amylose and hyperbranched amylopectin [13]. The amylose content in faba bean starch ranges from 29 to 40% [14–16]. The relatively high amylose content gives legume starches characteristic thermal properties such as restricted swelling capacity, high gelation temperature, more prominent aggregation and high final viscosity of gels [10, 12, 17]. Functional and physicochemical properties of pulse starches have been further explained by Singh [12].

The numerous chains in amylopectin are much smaller than the major chains found in amylose [18]. For faba bean amylose the degree of polymerisation (DP) is in the region of 1400 [17] and for amylopectin DP is 20.4 [16]. The amylose forms the amorphous and the amylopectin semi-crystalline granular regions. The radial arrangement of the crystalline amylopectin is believed to cause the birefringence patterns of starch under polarised light. The birefringence pattern for faba bean starch has been reported to be both strong and weak indicating disorganised amylopectin within the crystalline lamella [14, 15]. To further support this theory, scanning electron microscopy (SEM) imaging studies have revealed that faba bean starches are prone to cracking [14, 15] due to sub-optimal packing of starch chains, resulting in more fragile granules [14, 19].

Starch granules swell when heated in excess water because water molecules become linked by hydrogen bonding to the exposed hydroxyl groups of amylose and amylopectin and the crystalline structure is disrupted [12]. The

reported swelling patterns of faba bean starch are somewhat contradicting. Zhang, Tian, Wang, Jiang and Li [15] found that the swelling capacity of faba bean starches increased dramatically at temperatures surpassing 70 °C and progressively increased with temperature, likely due to increased molecular mobility. In another study swelling factor of faba bean starches progressively increased between 60 and 80 °C before declining beyond 85 °C [14]. Initially the presence of granular cracks facilitated the entry of water and increased amylose leaching. However, at temperatures beyond 85 °C the cracks reduced granular integrity therefore retarding the swelling. Compared to other pulse starches, solubility of faba bean starch was comparatively lower at 90 °C, also attributed to the granular integrity where restricted swelling and solubility were present [15].

The presence of granular cracks does not seem to have influenced the measured relative crystallinity of the faba bean starch (18–22%) [12, 13], which is within the reported crystallinity range (17–34%) of pulse starches [17]. Faba bean starches are classified to having the C-type polymorphic pattern; a combination of the more compact A-type pattern and more loosely packed B-type [20], which causes the the B-type polymorphs melt at lower temperature than the A-type [21].

During gelatinisation, starch undergoes from order to disorder phase transitions [17]. An observation from multiple studies [14–16] was that the enthalpy of gelatinisation ( $\Delta H$ ) for faba bean starch was in the lower end of the spectrum compared to other legumes. The gelatinisation temperatures ranged from 59 to 75 °C [11, 14–16] which was within the temperature gelatinisation spans reported for other legumes [17]. Li et al. [16] found that starches with a C-polymorphic pattern had lower  $\Delta H$  than A-type polymorphs. In the study by Ambigaipalan et al. [14] comparing C-type starches, the proportion of B-polymorphic content was not considered a factor influencing the gelatinisation properties. Instead, they [14] ratiocinated that the weakened crystalline structure of faba bean starch lowered the required  $\Delta H$ . Haase and Shi [22] who compared two varieties Chinese faba bean starches to a German one and found that the smaller German variety had a lower gelatinisation enthalpy.

For pasting to commence, starch granules need to be completely gelatinised [23]. During pasting the starch granules continue to swell with polysaccharides leaching out from the granules resulting in an increase of viscosity occurring during the shearing [12, 24]. Faba bean starch is reported to have high setback and final viscosity [11, 15, 16]. It is hypothesised that aggregation of leached amylose contributes to a strong-gelled network, which can reduce granular breakdown and maintain viscous gels. It is important to note that in each study [10, 13, 14] the heating profile of the rheological measurements was limited to heating the samples to the standard 95 °C. The shape of the obtained pasting curves

indicate that peak viscosity was not attained which could be contributing reason for the high setback and final viscosity. Amylose leaching has been reported to be much higher in faba beans (22%) compared to other bean sorts (black bean (15.5%) and pinto bean (16%)) [25]. The stability of starches is reflected in changes in viscosity during the heating process, while the changes occurring during cooling can predict the texture of the final products [11, 26]. Faba bean starches forming significantly stronger gels than other pulse starches lead Li et al. [16] to suggest that faba bean starch should be used for firm starch gel products such as glass noodles and jello-desserts.

In comparison to cereal starches, pulse starches tend to have a lower GI (glycaemic index) which can be beneficial when moderating insulin response and regulating the glucose metabolism [12]. The higher amylose content, C-type crystalline structure, resistant starch content and absence of pores on granular surfaces in pulse starches are associated with slower digestion rates, thereby improving the satiation effects of the foods [12, 27].

The aims of this study were to determine the chemical and structural composition of starches from Swedish faba bean cotyledon, faba bean hull, and to assess the influence of composition on the thermal properties. Wheat starch was used as a well-known Swedish sourced reference. Molecular size and structure were analysed by a combination of size exclusion chromatography (SEC) and nuclear magnetic resonance spectroscopy (NMR), while the polymorphic configuration of the lamella was measured using X-ray diffraction (XRD) and NMR. The granular swelling profile was visualised using microscopy and results were correlated with differential scanning calorimetry (DSC) measurements. The rheological profile was assessed using different heating profiles, up to 140 °C, and heating rates in a rapid viscosity analyser (RVA) and a rheometer. By comparing how the different heating parameters influence the measured viscosities, processes can be optimised to achieve desired products.

## Materials and methods

### Materials

Faba beans (*Vicia faba minor*) of the variety *Gloria* grown in central Sweden in 2016 were kindly provided by RISE in Uppsala, Sweden. The cultivar *Gloria* was chosen because it currently cultivated as a food crop due to lower tannin content [28]. The beans were dried until further use.

Prior to starch extraction, the beans were dehulled (Lu Cao Hi-tech Machinery, China). The hull and cotyledon fractions were then separately milled in a rotary mill (Barbender 880803, Duisburg, Germany) with mesh size 0.7 mm.

Starch from wheat, was used as a reference material and was kindly supplied by Lantmännen Reppe AB, Linköping W, Sweden. The reason for choosing wheat starch was because wheat is the most cultivated crop in Sweden [4], wheat starch can therefore be found in an abundance of products and has been widely studied.

### Hand-peeling: real ratio of cotyledon to hull in faba beans

To compare the ratio cotyledon to hull produced by the dehulling machine to the true ratio of the fractions, triplicate batches of 100 individual whole faba beans were immersed in distilled water at room temperature for 1 h. The beans were then peeled by hand. The cotyledon and hull fractions were dried separately at 105 °C and their relative proportions in total bean mass were calculated.

### Starch extraction

Starch extraction was based upon the extraction procedure of Lee [29] with some minor modifications. In brief, 200 g ± 1 g milled faba fractions cotyledons or hull were steeped in 1 L sodium hydroxide (NaOH) solution (0.02% w/v) for 24 h under continuous stirring at room temperature, and thereafter for a further 24 h without agitation at 4 °C. The bean matter was then separated from the NaOH solution by centrifugation (Thermo Scientific, Sorvall Lynx 4000, Waltham, MA, USA) at 3700×g for 5 min. The supernatant was removed and replaced with distilled water and the centrifugation process was repeated until pH 7 was reached.

After the final wash, the pellet was collected and mixed in a kitchen blender. The homogenised solution was filtered through a Büchner filter with a 70 µm nylon filter. To maximise starch extraction, these mixing and filtering steps were repeated. For starch recovery, the filtrate was left to stand without agitation overnight at 4 °C. The brown top layer of the starch was scraped off and the remaining starch was recovered and dried at 40 °C for 48 h. The dried starch was weighed and gently ground using a pestle and mortar. The starch samples were collected and stored in individual plastic bags for each extraction in a dry room until further analysis. In SEC and XRD measurements, starch from the early and late washing step were compared. However, due to scarcity of the material from the late washing, the extracted starch from each raw material was pooled for the remaining analyses.

All analysis were made in triplicate unless otherwise stated.

## Chemical composition analysis of starch

### Moisture content

To determine moisture content, 100 mg of samples was dried overnight at 105 °C (Heraeus UT12, Germany). The moisture content was calculated from the difference in mass before and after oven drying.

### Total starch and resistant starch

Total starch and resistant starch content were determined using the commercially available resistant starch kit (K-RSTAR 05/19, Megazyme International Ireland Ltd) according to AOAC Official Method 2002.02 [30].

### Amylose content

For determining the amylose content, the commercially available AM/AP assay kit (K-AMYL 06/18 by Megazyme International Ireland Ltd) was used with a method modified from Yun and Matheson [31].

### Ash content

For determining ash content, the AOAC Official Method 942.05 was followed.

### Protein content

Protein content was calculated from the nitrogen content ( $N \times 6.25$ ) measured by the Kjeldahl method [32], using a 2520 digester, Kjeltac 8400 analyser unit and 8460 sampler unit (all from Foss, Denmark).

### Fat content

Fat content was determined according to Commission Directive 152/2009 EC (2009) [33] using Hydrotec 8000 and Soxtec 8000 extraction units, both from Foss, Denmark.

Both the measured protein content and crude fat content for the wheat starch were calculated from single measurements, the standard deviation from the experiment control were 0.07 from raw protein and 0.14 from crude fat.

### Degree of branching

Degree of branching (DB) [34–36] was determined using  $^1\text{H}$  NMR spectroscopy. Starch samples (~10 mg) were placed in 5 mm NMR tubes, deuterated dimethyl sulfoxide ( $\text{DMSO-}d_6$ , 0.6 mL) was added and the mixture was kept at 80 °C overnight. To avoid spectral disturbance from hydroxyl proton signals, TFA- $d_1$  (10  $\mu\text{L}$ ) was added to the mixture just

before the NMR measurements [36]. The  $^1\text{H}$  spectra were recorded on a Bruker Avance III 600 MHz NMR spectrometer, using a 5 mm broadband observe detection smart probe equipped with z-gradient. The  $^1\text{H}$  spectra were acquired at 60 or 80 °C, using 128 scans with an acquisition time of 2.7 s and a relaxation delay of 12 s. The anomeric proton at the  $\alpha(1 \rightarrow 6)$ -linkage of the branching point, which has a different chemical shift than other anomeric protons, was used for quantification of DB. DB was calculated as the ratio  $I_{1-6}/(I_{1-6} + I_{1-4})$ , where  $I_{1-6}$  is the integrated signal at 4.8 ppm and  $I_{1-4}$  is the integrated signal between 5.0 and 5.2 ppm, corresponding to H1 of glucose at the  $\alpha(1 \rightarrow 6)$  and  $\alpha(1 \rightarrow 4)$ -linkages, respectively.

### Size exclusion chromatography (SEC)

Prior to the SEC analyses, intact branched starch samples were gelatinised and dissolved directly in SEC eluent consisting of dimethyl sulfoxide (DMSO, HPLC grade, Scharlab, Sweden) with 0.5% w/w LiBr (ReagentPlus) in a thermo-mixer at 80 °C with agitation. Enzymatic debranching of the starch molecules was performed with isoamylase (Megazyme, Ireland) in a 0.1 M acetate buffer (pH 3.5) at 37 °C for 4 h. After incubation, the samples were neutralised to pH 6.5–7.0, boiled to deactivate the enzyme, freeze-dried and redissolved in SEC eluent (DMSO with 0.5% w/w LiBr) for subsequent SEC analysis.

Separation of the intact starch samples and the debranched samples was performed in a SECcurity 1260 system (Polymer Standard Services, Mainz, Germany) coupled to a multiple-angle laser light scattering detector (MALLS; BIC-MwA7000, Brookhaven Instrument Corp., New York) and a refractive index detector (SECcurity 1260, Polymer Standard Services, Mainz, Germany) thermostatted at 45 °C, using a GRAM PreColumn, 30 and 3000 analytical columns (Polymer Standards Services, Mainz, Germany), with a flow rate of 0.5 mL  $\text{min}^{-1}$  at 60 °C.

Calibration of the SEC separation was performed using the Mark-Houwink relation by injection of pullulan standards provided by Polymer Standards Services (PSS, Mainz, Germany). The Mark-Houwink parameters for pullulan in DMSO/LiBr (0.5 wt%) at 80 °C are  $K = 2.427 \times 10^{-4} \text{ dL g}^{-1}$  and  $a = 0.6804$  [37]. Data treatment and collection were performed using WinGPC software (Polymer Standards Services, Mainz, Germany) and the data were further analysed by additional mathematical procedures presented elsewhere [37]. The differential index of refraction ( $\text{dn}/\text{dc}$ ) for starch in DMSO/LiBr 0.5% was taken to be 0.0544 mL  $\text{g}^{-1}$  [37]. Different molecular parameters and distributions, including SEC weight distribution ( $w(\log V_h)$ ), branch chain-length distribution ( $w(\log X_{de})$ ) and size dependence of the weight-average molecular weight ( $M_w(V_h)$ ), were thus obtained. The

macromolecular size distributions are presented in terms of hydrodynamic radius ( $R_h$ ), with  $V_h = 4/3 \pi R_h^3$ .

### X-ray diffraction (XRD)

The XRD measurements were performed using a Panalytical X'pert Pro operating at 45 kV and 44 mA, with Cu K $\alpha$  radiation. Diffraction patterns were recorded using a radiation wavelength of 1.54 Å. The runs were duplicated for each sample. The crystallinity ratio was determined by the Rietveld method [38]. The crystalline peaks were resolved from the amorphous halo and the relative crystallinity was obtained as the area of the crystalline peaks divided by the total intensity area within  $2\theta$  of 3°–40° [39, 40].

### $^{13}\text{C}$ CPMAS NMR

$^{13}\text{C}$  cross-polarisation (CP) magic angle spinning (MAS) NMR spectra were obtained on a Bruker Avance III 600 MHz spectrometer using a double-resonance 4 mm ( $^1\text{H}$ & $^{19}\text{F}$ )/( $^{15}\text{N}$ - $^{31}\text{P}$ ) CP-MAS probe. Starch samples (~80 mg) were packed into 4 mm ZrO $_2$  rotors and the CPMAS spectra were recorded at 25 °C, using a spinning frequency of 12 kHz, a contact time of 1–2 ms and a repetition delay of 2.5–5 s. The amount of water in the dried starch samples was: cotyledon 7.5%, hull 8.6% and wheat 9.5%.

### Light microscopy

Starch granules were suspended in 50% (v/v) glycerol/water and aliquots of the starch slurry were pipetted onto a glass slide. To emphasise contrast and granular structure for brightfield microscopy, granules were stained with dilute Logulus/water solution (50% v/v) prior to sealing with a cover slip. Samples were examined under polarized light and differential interface contrast (DIC) was prepared in the same manner as for brightfield microscopy, with the exemption of the Logulus staining. All observations were performed using a light microscope (Nikon Eclipse Ni-SSR 930151, Tokyo, Japan) with objective PlanApo 20 $\times$  (0.75 N.A.) and PlanApo 40 $\times$  (0.95 N.A.). Images were recorded with a Nikon Digital Sight DS-Fi2 camera (Nikon, Tokyo, Japan) with resolution of 2560 $\times$ 1920 pixels.

For image analysis, the micrographs were thresholded in Fiji/ImageJ. To reduce noise, the limitation settings for the images were minimal size 2  $\mu\text{m}^2$  and circularity 0.2. The programme was set to exclude granules on the micrograph edges.

To calculate average length and width, an ellipse was fitted for each individual granule.

### Hot-stage microscopy

A 1 mg sample of starch was suspended with 1 mL distilled water using a vortex mixer, 80  $\mu\text{L}$  of the starch–water slurry were pipetted onto a cover slip and 15  $\mu\text{L}$  of diluted Logulus stock solution were added to dye the starch. The specimen was then observed using brightfield microscopy. A smaller cover slip was placed on top and the sample was sealed with nail polish. For birefringence analysis using polarised light, samples were not stained with Logulus solution.

A tensile-stage Linkam (model TST350, Linkam Scientific Instruments, Surrey, UK) with heating capacity was attached to the light microscope (Nikon Eclipse Ni-SSR 930151, Tokyo, Japan). Samples were observed under both polarized and brightfield light, using objective Plan Fluoro 10 $\times$  (0.30 N.A.). Because of the working distance of objectives, higher magnifications were not possible.

The heating rate was 5 °C/min within the range 25–95 °C. A sequence of images (2560 $\times$ 1920 pixels) was captured with a microscope camera (Nikon, DS-Fi2, Tokyo, Japan) every 12 s, i.e. at each 1 °C temperature interval.

All the acquired images were visually analysed and compared, to pinpoint the temperature at which major granular changes were observed. From 40 to 75 °C at 5 °C intervals, the images were analysed as previously described for light microscopy, using Fiji/ImageJ.

### Scanning electron microscopy (SEM)

The starch granules were also analysed by SEM (Hitachi TM-1000, Tokyo, Japan) at an accelerating voltage 15 kV, with an image size of 2560 $\times$ 1920 pixels. Carbon tape with the evenly dispersed starch samples was mounted on an SEM stub and sputter coated with Au (Cressington Scientific Instruments, Sputter coater-108 auto, Watford, UK).

### Differential scanning calorimetry (DSC)

Gelatinisation characteristics of starch thermal properties were measured using a Mettler Toledo DSC1. Starch samples  $3 \pm 1$  mg and  $12 \pm 1$   $\mu\text{L}$  distilled water were placed in aluminium pans and sealed hermetically (MT no. 51119872). The sealed pans were allowed to stand overnight at room temperature in order to achieve uniform distribution of water before DSC analysis. The samples were scanned from 30 to 200 °C at a rate of 10 °C/min. A thermogram was recorded with an empty aluminium pan as reference and the blank pan value was subtracted from all measurements. The sample chamber was flushed with inert gas (nitrogen, purge rate 50 mL/min) during the scan.

## Rheological measurements

A Rapid Visco Analyzer (RVA, Newport Scientific, Warriewood, NSW, Australia) and a rheometer (HR-3, Discovery Hybrid Rheometer, New Castle, DE, USA) were used to analyse, measure and compare the rheological properties of the different starches depending on heating rate, temperature ranges and which instrument was used.

### Rapid Visco Analyzer (RVA)

In the RVA the pasting properties were determined at two different heating rates, 12 °C/min and 1.5 °C/min. For both experimental set-ups, 2 g starch were mixed with 25 mL distilled water. The paddle rotation was 960 rpm for the first 10 s, then constant at 160 rpm for the remainder of the experiment. The samples were equilibrated at 50 °C for 1 min before heating to 95 °C. With heating rate 12 °C/min, the samples were kept at maximum temperature (95 °C) for 2.5 min before cooling at 12 °C/min to 50 °C and held at the final temperature for 2 min. With heating rate 1.5 °C/min, the heated starch mixtures were kept at maximum (95 °C) temperature for 5 min and final (50 °C) temperature 2 min. The interval between viscosity and temperature readings was 4 s. For microscopy analysis, smears of the pastes were made on microscope slides immediately after each run.

### Rheometer

Rheology data were obtained using the rheometer equipped with a Peltier pressure cell and steel starch paddle. Two different heating cycles, 50–95–50 °C and 30–140–30 °C, both with a heating rate of 1.5 °C/min, were applied in triplicate to each starch type. Before cooling at the same rate (1.5 °C/min), the samples were held at maximum temperature for 5 min. The rotational speed for the initial 20 s was the device's maximum, i.e. 50 rad/s (477.5 rpm), and then for the remainder of the experiment it was 16.75 rad/s (160 rpm). To mimic the concentration of the starch slurry in the RVA measurements, 2.08 g of starch were mixed with 26 mL distilled water. For microscopy analysis, smears of the pastes were made on glass slips immediately after each run.

### Statistical analyses

Statistical analyses were carried out in Excel and Rstudio (Version 1.2.5033, RStudio Inc., MA, USA). One-way and two-way ANOVA with Pearson correlation coefficients and density plots using ggplot2 were created in R.

## Results and discussion

### Chemical composition

The ratio of cotyledon to hull and the starch content of the hull fraction differed depending on the method used for fraction separation. When the beans were peeled by hand, the cotyledon fraction represented  $88.4 \pm 0.2\%$  and the hull fraction  $11.6 \pm 0.2\%$  of the whole faba bean mass, and the measured starch content of the hull was negligible ( $0.004 \pm 0.00\%$ ). However, when the beans were peeled by machine, the ratio of cotyledon to hull was estimated to be 78 to 22, and the measured starch content of the hull was  $19.1 \pm 0.6\%$  [41]. Therefore, it is likely that part of the hull starch analysed in this study was actually starch from the outer layers of the cotyledon. During the machine-dehulling the embryo location was not taken into consideration.

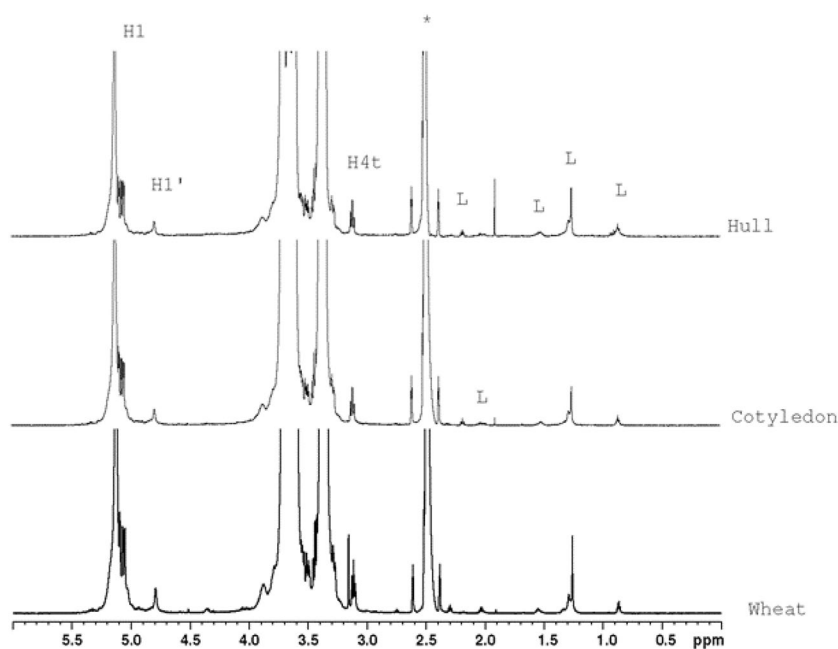
The chemical composition of starch from the cotyledon, hull and wheat samples is summarised in Table 1, the composition of the cotyledon starch was in accordance with literature values [11, 14–16, 22, 29]. The starch extracted from faba bean hull contained significantly more protein and ash as well as more fat, than the other two starches, possible due to the presence of the embryos. The wheat starch contained significantly lower amounts of amylose (21%) compared with the faba bean starches (hull 36%, cotyledon 32%) (Table 3).

The quantity of resistant starch was greatest in the hull (13.1%), followed by the cotyledon (6.7%), while wheat starch contained negligible amounts of resistant starch (0.5%). Resistant starch is defined as the starch that can resist  $\alpha$ -amylase hydrolysis in the small intestine and is therefore available for fermentation in the large intestine [42, 43].

### Degree of branching

To our knowledge, measuring the degree of branching (DB) in faba bean starch using  $^1\text{H}$  NMR is a new feature where comparable values could not be found in literature. Based on the  $^1\text{H}$  NMR spectra (Fig. 1), DB of cotyledon, hull and wheat starch was determined to be 4.1, 4.2 and 4.7%, respectively. The slightly higher DB of wheat starch correlates well with its lower amount of amylose. Previous studies have shown that wheat starch has a low level of branching, with  $\alpha$ -(1,4)/ $\alpha$ -(1–6) ratio of around 21. Signals from lipids were clearly observed in the  $^1\text{H}$ -NMR spectra of, hull, cotyledon and wheat starch samples (Fig. 1), with the profile being slightly different in wheat starch compared with the hull and cotyledon starches.

**Fig. 1**  $^1\text{H}$  NMR spectra of starch from wheat starch and from faba bean cotyledon and hull. Glucose H1 at the  $\alpha(1 \rightarrow 4)$ -linkage (H1) and at the  $\alpha(1 \rightarrow 6)$ -linkage (H1') is indicated, as is H4 of non-reducing end terminal residues (H4-t). Beside the H1 and H4 signals from glucose in starch, (L) signals corresponding to lipidic protons are also indicated. \*Deuterated dimethyl sulfoxide (DMSO)



## Molecular size and degree of polymerisation (DP)

Figure 2 shows the size distributions,  $w(\log V_h)$  and absolute molecular weight ( $M_w$ ) of intact branched starch molecules as a function of their hydrodynamic radius ( $R_h$ ). A typical bimodal distribution was observed for all starch types, corresponding to the amylose ( $R_h$  10–100 nm) and amylopectin ( $R_h$  100–1000 nm) populations. The absolute molar mass values from light scattering (MALLS) detection were comparable, with average values for the amylose and amylopectin populations in the faba bean cotyledon and hull starches of 10–20 MDa and 60–100 MDa, respectively. These were slightly lower molar masses than in the reference wheat starch. There were no significant differences between the early and late washing faba bean samples.

In the branch chain length distributions as a function of the degree of polymerisation (DP) after enzymatic debranching (Fig. 3), there were two evident peaks for all starches, with a cut-off at around DP 100 in the SEC graphs. Others have identified DP 100 as the cut-off point for amylopectin and amylose [44].

Wheat starch contained proportionately more short-chain amylopectin (DP 6–12) and very-short-chain amylopectin (DP < 6). The branch-chain length distribution was similar for the faba bean cotyledon and hull starches, but the DP distribution for the faba bean starches differed from previously reported values [14, 16] in that they contained a smaller proportion of  $\text{DP} \leq 24$ . Correlation between degree of branching and high prevalence of short chain amylopectin was strong, respectively  $\text{DP} < 6$  ( $r = 0.99$ ;  $p < 0.001$ ),  $\text{DP} 6\text{--}12$  ( $r = 1.00$ ;  $p < 0.001$ ) and  $\text{DP} > 37$  ( $r = -1$ ;  $p < 0.001$ ). No statistically significant correlation was found between

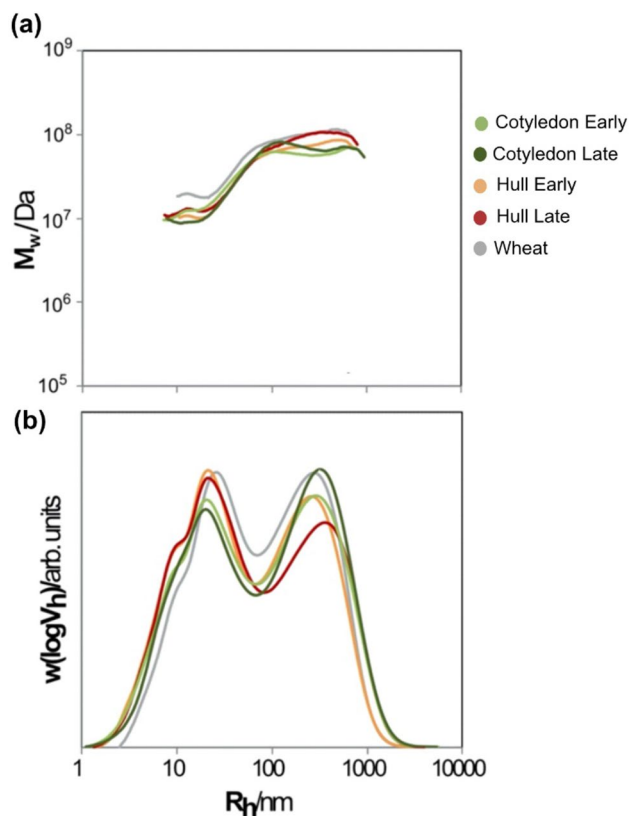


**Fig. 2** Distribution of (a) absolute molecular weight [ $M_w/\text{Da}$ ] and (b) size exclusion chromatography (SEC) weight [ $w(\log V_h)$ ] of intact branched starch molecules as a function of the hydrodynamic radius [ $R_h/\text{nm}$ ]. Amylose  $< [R_h/\text{nm} < 100] <$  amylopectin. ‘Early’ and ‘Late’ refer to washing steps

**Table 1** Chemical composition (dry weight basis) of starch extracted from faba bean cotyledon and hull and from wheat grain (mean ± standard deviation)

Samples	Chemical composition, %					
	Total starch	Amylose *	Resistant starch*	Protein	Fat	Ash
Cotyledon	95.5 <sup>b</sup> ± 0.3	32.2 <sup>b</sup> ± 0.8	6.7 <sup>b</sup> ± 0.3	0.55 <sup>a</sup> ± 0.08	0.32 <sup>a</sup> ± 0.03	0.18 <sup>a</sup> ± 0.01
Hull	93.6 <sup>a</sup> ± 0.8	36.0 <sup>c</sup> ± 0.9	13.1 <sup>c</sup> ± 1.1	2.8 <sup>b</sup> ± 0.6	0.53 <sup>a</sup> ± 0.04	0.46 <sup>b</sup> ± 0.01
Wheat	99.0 <sup>c</sup> ± 0.3	21.2 <sup>a</sup> ± 0.8	0.50 <sup>a</sup> ± 0.07	0.2 <sup>a</sup> ± NA	0.40 <sup>a</sup> ± NA	0.15 <sup>a</sup> ± 0.01

NA not applicable (the SD from the experiment control were; ±0.07 raw protein and ±0.14 crude fat)

The superscript lower-case letters signify statistical significant difference compared in each column

\*Percentage of total starch

amylopectin molecular weight or hydrodynamic radius with either degree of branching or prevalence of a specific DP.

The most interesting difference between the faba bean starches and the reference wheat starch was in terms of amylose branches. Both faba bean starches showed a bimodal branch chain length distribution for amylose, with two populations centred around DP 700 and DP 2500. In all faba bean samples, the larger branch population (centred around DP 2500) in amylose was more abundant than the smaller (centred around DP 700). On the contrary, wheat starch showed a larger abundance of the shorter amylose branches (centred at DP 1100) than of the longer branches (centred at DP 2500).

**X-ray diffraction (XRD)**

In the X-ray diffraction spectra of the different starches (Fig. 4), the faba bean cotyledon and hull starches both displayed spectra typical for C-type starches, whilst the spectra for wheat starch resembled the A-type pattern. The hull and wheat starches, but not the cotyledon starch, exhibited low intensity peak at 2θ=20° (Fig. 4), indicating the presence of V-type amylose lipid complex [45].

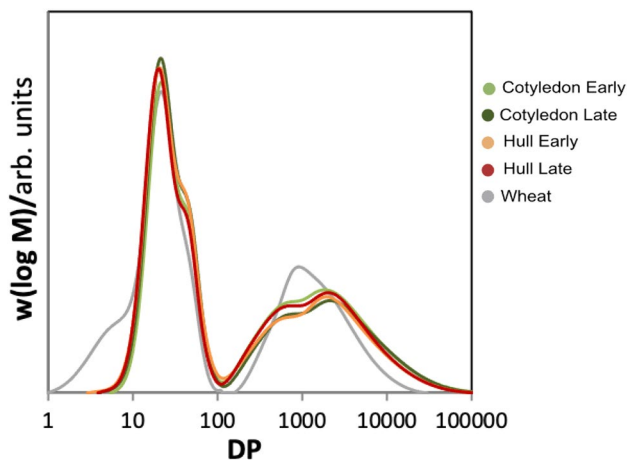


**Fig. 3** Branch chain length of the starch i.e. SEC molecular weight [w(logM)] as a function of degree of polymerisation (DP) distribution amylopectin < [DP 100] < amylose

The relative crystallinity was highest for wheat starch (18.6%). In both faba bean starches, the relative crystallinity was lower in samples extracted in the late washing (cotyledon 16.4%, hull 16.7%) than in the early washing (cotyledon 17.6%, hull 17.5%). For all samples the relative crystallinity was comparatively lower than previous reports i.e. for wheat (27–36%) [46] and faba 20–22% [14, 15]. Amylose content was negatively correlated ( $r = -0.747$ ;  $r < 0.05$ ) with relative crystallinity, which could be attributed to the fact that amylopectin makes up the semi-crystalline region, whereas amylose is present in the amorphous form [16, 18, 47, 48]. A negative correlation between relative crystallinity and amylose content has been reported previously for a range of legume starches [50].

**<sup>13</sup>C CPMAS NMR**

The <sup>13</sup>C CPMAS NMR spectra for the cotyledon, hull and wheat starches are shown in Fig. 5, with the assignment of the C1 to C6 resonances of the glucose-repeating unit indicated at the top of the spectra. The C1 region commonly used to analyse the structure of different types of starch

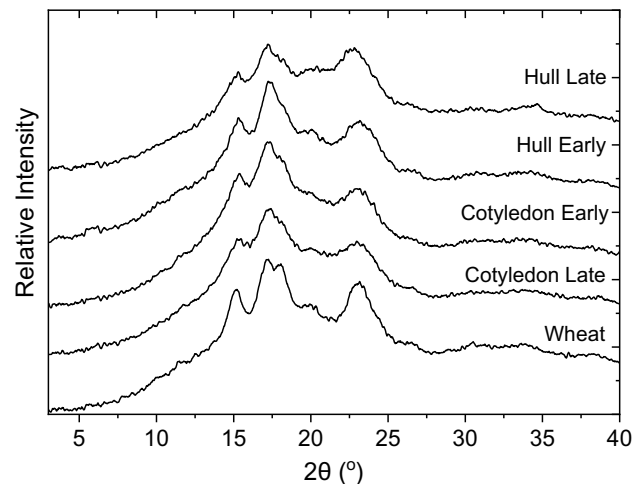


**Fig. 4** Wide-angle X-ray powder diffraction spectra of hull starch, cotyledon starch and wheat starch. Strong singlet peaks at 17° and 23° 2θ indicate C-type polymorph for the faba bean starches; hull and cotyledon. Doublet peak at 17–18° 2θ and strong peaks at 15° and 23° 2θ in wheat indicates A-type polymorph [49, 50]

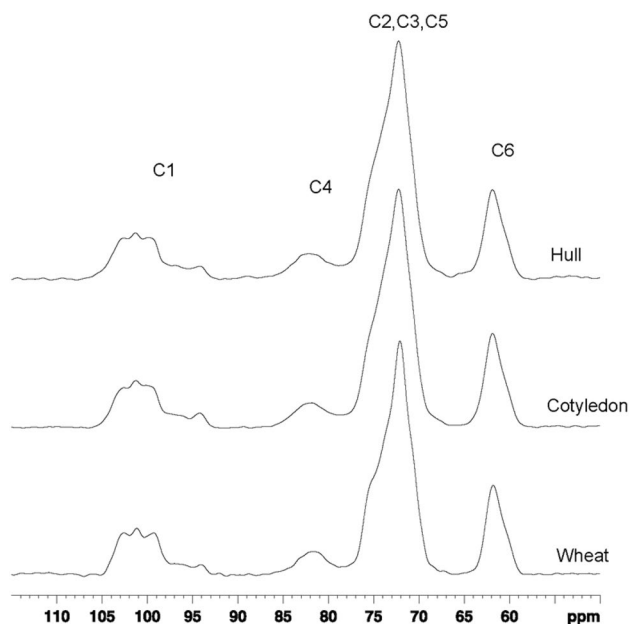


**Fig. 5**  $^{13}\text{C}$  CP/MAS NMR spectra of wheat, faba bean cotyledon and faba bean hull starches with resolution-enhanced apodization (GB=0.1, LB=-100)

[51–55] exhibits signals from amorphous and crystalline starch with chemical shifts between 93.9 and 105.2 ppm. The C1 signal in wheat starch showed the distinct three-peak pattern characteristic of crystalline A-type starch. For B-type starch, the C1 signal is a doublet, while for C-type starch it is a mixed pattern of both A- and B-types. In general, the C1 signal appears as a triplet if the A-crystalline structure is predominant and as a doublet if the B-type is predominant. Thus, the cotyledon starch had a pattern more similar to that of C-type starch with a predominance of A-type, for the hull starch the triplet pattern was even more nuanced. An interpretation of both the XRD and NMR-spectra of the hull starch could be that the hulls starch also displays the polymorphic-pattern  $C_{A-}$  type (closer to A type), as previously observed by Cai, Cai, Man, Zhou and Wei [55]. The broad resonances in the C1 region together with the broad C-4 signal around 80–84 ppm represent amorphous starch (Fig. 4). The signal at 93.9 ppm was present in all CPMAS spectra and was not much broader than the signals from crystalline starch. This signal has been observed in CPMAS NMR spectra of many different types of starch, and has recently been tentatively attributed to constrained conformations [56].

### Granular morphology

The size range of the different starch granules at room temperature is shown in Table 2. Mean length and mean width of the cotyledon starch were both larger than for the hull starch, the cotyledon starches were also more uniform in size, with a smaller standard deviation.

**Table 2** Granule length and width (mean  $\pm$  standard deviation) of faba bean cotyledon starch, faba bean hull starch and wheat starch as measured by light microscopy

Sample	Length $\mu\text{m}$		Width $\mu\text{m}$	
Cotyledon	22.8 <sup>d</sup> $\pm$ 6.7		17.1 <sup>d</sup> $\pm$ 4.3	
Hull	21.3 <sup>c</sup> $\pm$ 6.7		15.8 <sup>c</sup> $\pm$ 4.7	
Wheat	A	B	A	B
	19.8 <sup>b</sup> $\pm$ 6.1	7.0 <sup>a</sup> $\pm$ 1.5	15.2 <sup>b</sup> $\pm$ 5.1	6.7 <sup>a</sup> $\pm$ 1.6

The superscript lower-case letters signify statistical significant difference

In both the cotyledon (a2–a5 in Fig. 6) and hull (b2–b5) starches, granule shape varied between ellipsoidal and irregular. In the SEM micrographs, evident cracks were present on granule surfaces for both faba bean starches. The wheat starch (panels c2–c5 in Fig. 6) was composed of both larger A ( $> 10 \mu\text{m}$ ) and smaller B ( $< 10 \mu\text{m}$ ) granules. The wheat starch granules were either round or ellipsoidal, with visible pits or craters on the surface (indicated by chevrons in Fig. 6c). These type of structures are reported to be caused presumably by enzymatic reactions [57].

Panels a3, b3 and c3 in Fig. 6 show the birefringence of starch granules in faba bean cotyledon, faba bean hull and wheat starch, respectively. The birefringence patterns of faba bean granules was both strong and weak, which is consistent with literature values [14]. A less defined Maltese cross was seen for the faba bean samples, presumably due to suboptimal packing of the amylopectin owing to weak interactions between the chains [11, 19] caused by large deviations in amylopectin DP preventing optimal packing of double helical segments [58]. Interestingly, granules displaying weak birefringence patterns had cracks on the surfaces (see arrows in panels a3–a5 & b3–b5 in Fig. 6).

### Thermal transitions-granular swelling

Figure 7 shows the size distribution of starch granules at different temperature intervals between 30 and 70 °C measured during the hot-stage microscopy. The microscopy images were separately analysed at 1 °C intervals in order to see more precisely at which temperatures major changes were observed. The size of cotyledon starches (Fig. 7a) started to increase at 61 °C and the greatest increase in size was between 65 and 66 °C, followed by the granules becoming more translucent and merging.

The hull starch (Fig. 7b) was the most heat-tolerant of the three starches, as the granules retained their shape and resisted swelling. For the hull, the most dramatic increment in size was observed between 71 and 72 °C. At 73 °C, the granules became more translucent with jagged edges.

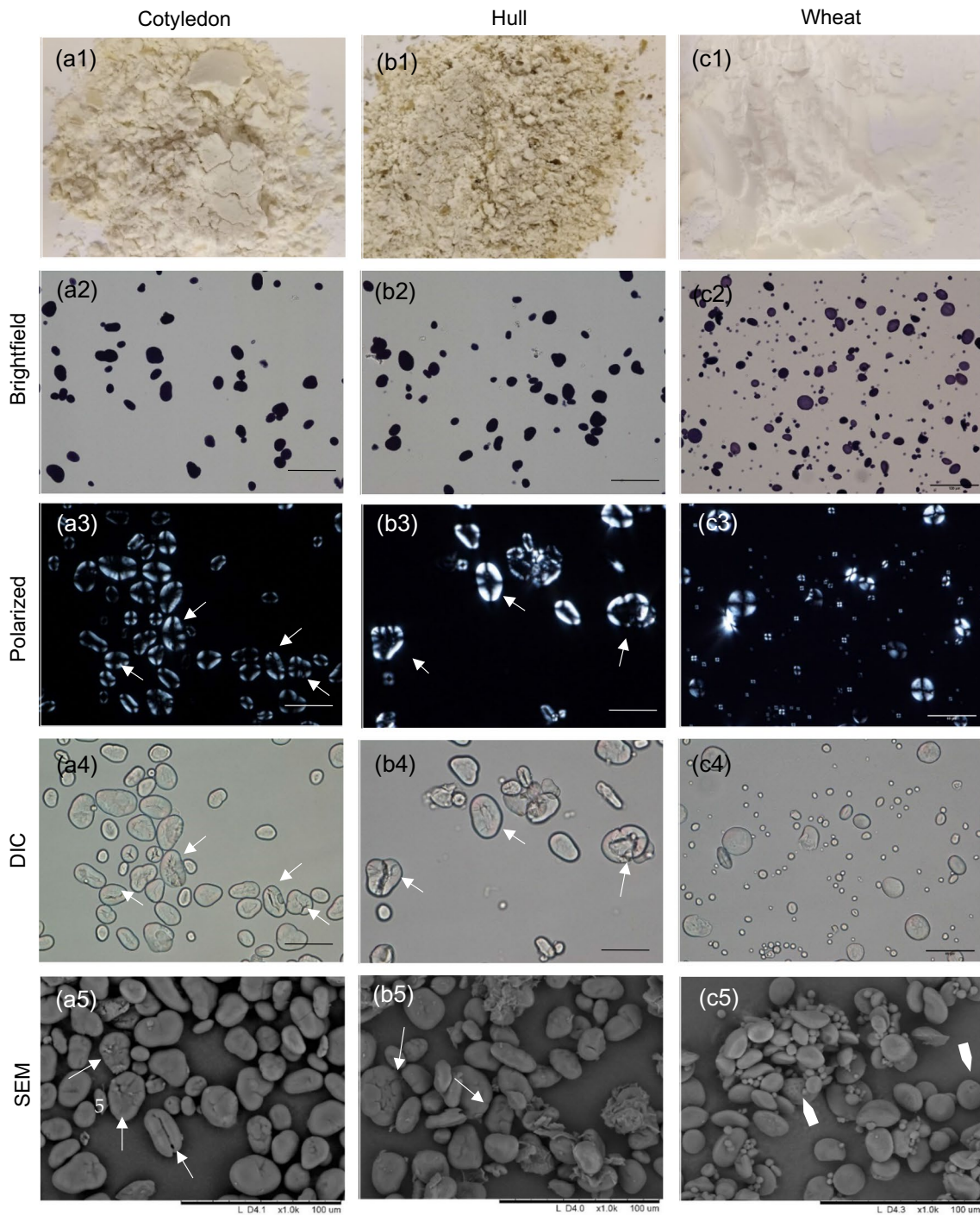


**Fig. 6** (a) cotyledon starch; (b) hull starch; (c) wheat starch; (1) Normal photograph; (2) light microscope micrograph; (3) polarized light micrograph; scale bar=100 μm; (4) differential interface contrast (DIC) micrograph; scale bar=50 μm (5) and scanning electron micrograph; scale bar=50 μm. Arrows indicate cracked granules; chevrons indicate surface pitting

trast (DIC) micrograph); scale bar=50 μm (5) and scanning electron micrograph; scale bar=50 μm. Arrows indicate cracked granules; chevrons indicate surface pitting

The wheat starch (Fig. 7c) was the least heat-tolerant of the three starches. Swelling initiated at 53–54 °C, while a dramatic increase in size was observed at 57 °C.

completely lost at 71 °C for the hull, 62 °C for the cotyledon and 58 °C for the wheat.

Loss of birefringence can be considered as an indicator that the starch has fully gelatinised. Birefringence was

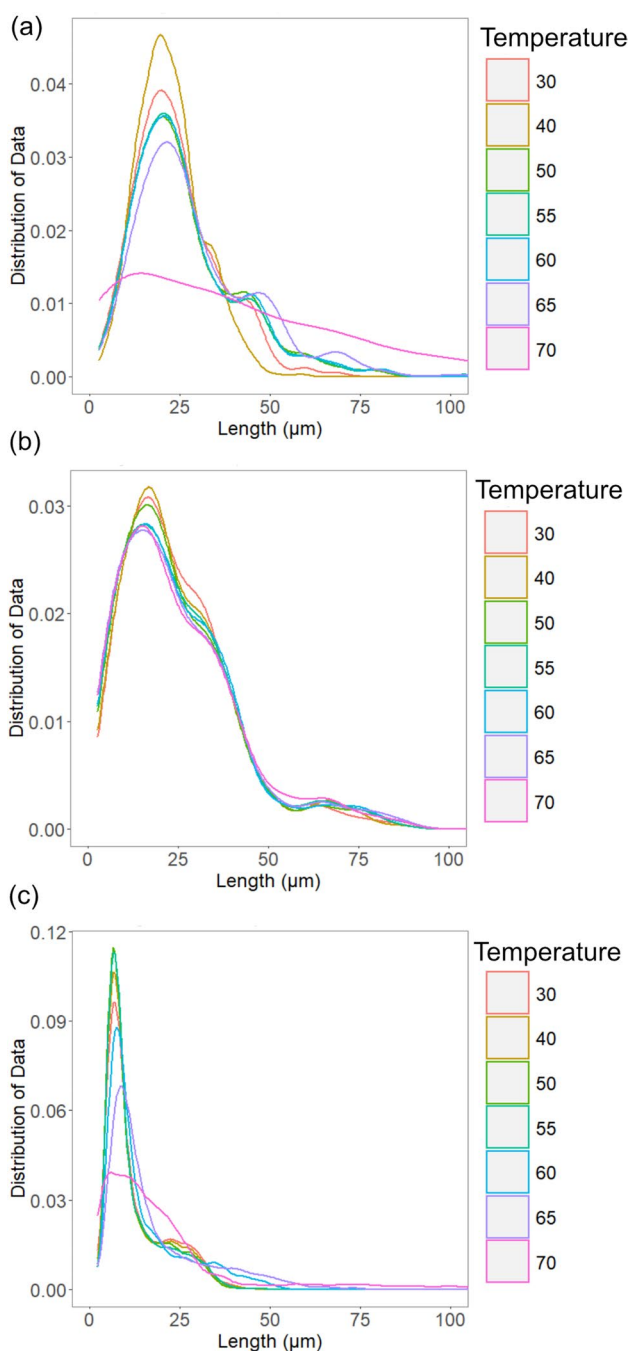


**Fig. 7** Density diagrams showing along the x-axis the starch granular length and along the y-axis the distribution of granules within population at different temperatures. **a** Faba bean cotyledon starch; **b** faba bean hull starch and **c** wheat starch during progressive heating from the hot-stage microscopy

### Thermal transitions- gelatinisation temperatures

Thermal transition temperatures recorded during the DSC ranked the starches in the order hull > cotyledon > wheat (Table 3). The temperatures recorded for the phase transitions in DSC were in accordance with the changes in

**Table 3** Thermal transition temperatures (mean  $\pm$  standard deviation) recorded by differential scanning calorimetry (DSC)

Sample	$T_o$ ( $^{\circ}\text{C}$ ) <sup>1</sup>	$T_p$ ( $^{\circ}\text{C}$ ) <sup>2</sup>	$T_c$ ( $^{\circ}\text{C}$ ) <sup>3</sup>	$\Delta\text{H}$ (J/g) <sup>4</sup>
Cotyledon	67.2 <sup>b</sup> $\pm$ 0.1	69.4 <sup>b</sup> $\pm$ 0.1	72.7 <sup>b</sup> $\pm$ 0.3	7.4 <sup>b</sup> $\pm$ 0.3
Hull	70.0 <sup>a</sup> $\pm$ 0.1	72.4 <sup>a</sup> $\pm$ 0.2	75.5 <sup>a</sup> $\pm$ 0.2	7.6 <sup>b</sup> $\pm$ 0.2
Wheat	57.6 <sup>c</sup> $\pm$ 0.2	61.1 <sup>c</sup> $\pm$ 0.1	64.9 <sup>c</sup> $\pm$ 0.1	9.5 <sup>a</sup> $\pm$ 0.2

The superscript lower-case letters signify statistical significant difference.

<sup>1</sup>Onset temperature

<sup>2</sup>Peak temperature

<sup>3</sup>Endset or conclusion temperature

<sup>4</sup>Enthalpy change

granular structure observed by hot-stage microscopy (Fig. 7). The onset gelatinisation temperature for both faba bean starch samples was higher than in previous reported studies (range 57–65  $^{\circ}\text{C}$ ), but the endset temperature was more similar to that reported previously (72–75  $^{\circ}\text{C}$ ) [14–16, 29]. Despite the narrower gelatinisation temperature range for the faba bean samples in this study, the enthalpy of gelatinisation for the hull and cotyledon starches was within the reported range [14–16, 29].

Correlation between gelatinisation temperature and amylose content was strong ( $r = 0.99$ ;  $p < 0.001$ ). The hull starch, with the highest amylose content, had the most restricted swelling pattern and highest gelatinisation temperature, while the wheat starch, with the lowest amylose content, displayed the lowest gelatinisation temperature. Amylose retards initial swelling by imposing a stabilising effect on the granular structure [59].

The peak temperature during gelatinisation reflects the crystallite quality, while the gelatinisation enthalpy is a reflection of the overall crystallinity and an indicator of the loss of molecular order within the granule [55]. There was a strong negative correlation between gelatinisation temperature and abundance of very short amylopectin chains, ( $r = -0.97$ ;  $p = 0.006$ ). It is possible that the higher prevalence of short-chain amylopectin in the wheat reduced the gelatinisation temperature, as the so-called “fingerprint” amylopectin chains (DP 6–8, see Fig. 3) are too short to form double helices and instead cause crystalline defects, which could facilitate the entry of water [19, 20].

The DSC curve (available in supplementary material) of wheat starch exhibited a wider peak than that of the bean samples. This coincided with a wider gelatinisation temperature range (7.3  $^{\circ}\text{C}$ ) for wheat starch compared with both faba bean starches (5.5  $^{\circ}\text{C}$ ). The enthalpy of gelatinisation was higher for wheat starch (9.5 J/g) than for cotyledon starch (7.4 J/g) and hull starch (7.6 J/g). The wheat starch contained two distinct granule populations

(see Table 2 and Fig. 6), which could be the reason for the broader gelatinisation range [60].

**Pasting**

Figure 8 shows pasting curves for heating profile 50–95–50 °C in: RVA with heating rate 12 °C/min (a), RVA with heating rate 1.5 °C/min (b) and rheometer with heating rate 1.5 °C/min (c) and heating profile 30–140–30 °C in rheometer with heating rate 1.5 °C/min (d). It was the striking difference between the shape of the pasting curves and viscosities values of the 12 °C/min

RVA pasting curve (Fig. 8 a) and rheometer pasting curve with heating profile 30–140–30 °C (Fig. 8d), that sparked the investigation to compare the RVA (Fig. 8b) with the rheometer (Fig. 8c) using the same parameters.

The general shape of the pasting curves with the heating profile 50–95–50 °C (Fig. 8; a-c) was similar, with cotyledon starch forming pastes with the highest viscosity, hull starch the second highest viscosity and wheat starch the lowest viscosity. The pasting curves in Fig. 8b and c had the same heating rate of 1.5 °C/min whilst the pasting curve in (Fig. 8a) was the fastest with 12 °C/min. The cotyledon starch began to paste first, at around 77 °C, followed by

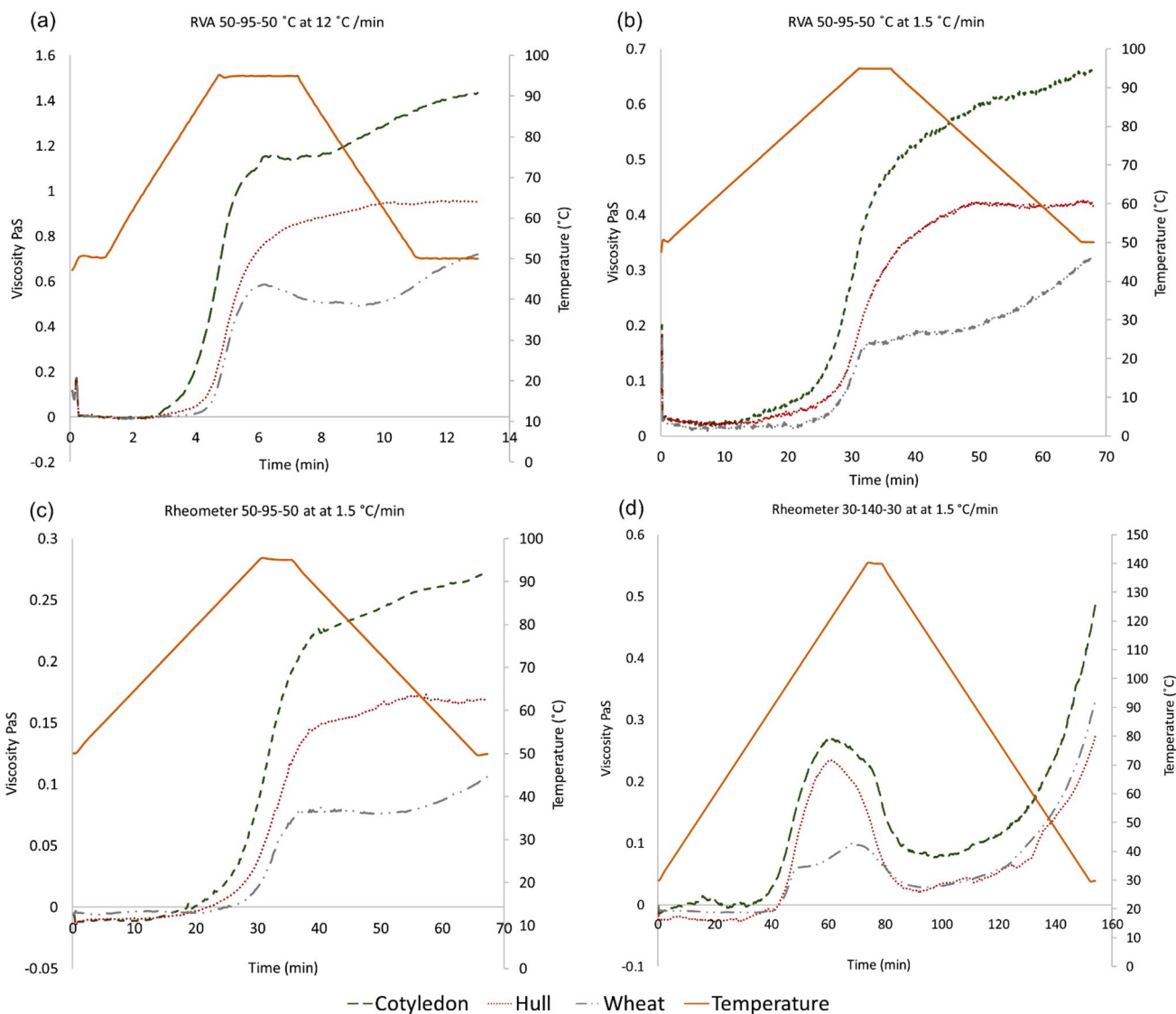


**Fig. 8** Pasting curves of faba bean cotyledon starch, faba bean hull starch and wheat starch; **a** Rapid viscosity analysis (RVA) heating profile 50–95–50 at heating rate 12 °C/min; **b** RVA heating profile 50–95–50 at heating rate 1.5 °C/min; **c** rheometer heating profile 50–95–50 at heating rate 1.5 °C/min; **d** Rheometer heating cycle

30–140–30 °C at heating rate 1.5 °C/min. Please note the different viscosity ranges (Pa S) for each pasting graph. In the supplementary material pasting graphs of the same data can be found, only difference is that the Viscosity ranges (Pa S) are the same for all graphs

hull starch (85 °C) and wheat starch (94 °C). The cotyledon and hull starches both displayed the common characteristics of legume starches, i.e. high pasting temperature, absence of peak viscosity, increasing viscosity during the holding period and high set-back (Fig. 8a–c). This in agreement with previous findings for pulse starches [17].

Higher prevalence of longer amylopectin chains and amylose chains was correlated with higher pasting viscosity ( $r = 0.99$ ;  $p = 0.001$ ). The abundance of amylopectin chain with  $DP < 6$  in the wheat starch may have further lowered the relative viscosity ( $r = -0.97$ ;  $p = 0.008$ ). The theory is that longer amylopectin chains have the ability to interact with the amylose chains, increasing the aggregation viscosity [44]

The final viscosity for the RVA with a heating rate at 12 °C/min was on average 2.2 times higher than the final viscosity for the same starch when the heating rate was 1.5 °C/min in the RVA and 5.9 times higher than the values measured with the rheometer. A correlation between swollen granular size and peak viscosity after heating cycle 50–95–50 °C was observed ( $r = 0.73$ ;  $p < 0.025$ ). The swollen starch granules in the smear micrographs (see Fig. 9) with heating rate 12 °C/min (Fig. 9a1–c1) were on average 1.3 times larger than when the heating rate was 1.5 °C/min for both the RVA (Fig. 9a2–c2) and the rheometer (Fig. 9a3–c3). Suspensions with larger starch granules have

previously been reported to exhibit higher viscosities [45, 61, 62].

As the RVA consistently measured higher viscosities than the rheometer, possibly due to water evaporation because the RVA is not a fully sealed system, shows that the instruments are not interchangeable.

When using instruments for estimating rheological properties of different food products produced at an industrial scale, an important consideration will be how much material is heated, at what pace and how sealed the heating vessels are.

Heating the samples to 140 °C, which is a much higher temperature than the standard 95 °C, was sufficient for the faba bean starches to achieve peak viscosity, at 119 °C for cotyledon starch and 121 °C for hull starch, followed by an evident viscosity break-down (Fig. 8d). For the wheat starch there appeared to be two peaks, a first smaller peak at 104 °C and a second more pronounced peak at 132 °C, with the first peak presumably reflecting amylopectin melting and the second peak reflecting melting of amylose lipid complexes [63, 64]. Peak viscosity reflects the swelling intensity [65]. Breakdown viscosity occurs because of granule rupture, which induces loss of paste viscosity [66]. In terms of final viscosity, the cotyledon paste was significantly more viscous ( $p = 0.003$ ) than the hull and the wheat starch pastes, while the hull paste was slightly less viscous than the wheat paste, possibly because of disintegration of the granules (Fig. 9a4–c4).

Interestingly, at lower heating temperatures, the hull starch appeared most heat-stable but at very high temperatures, the hull starch produced the softest gels. Comparing the smears from all heating cycles (Fig. 9) the starch granules heated to 95 °C (a1–c3) appear much more intact with low leakage of amylose compared to the smears after heating samples to 140 °C (a4–c4). A negative correlation was found between the pasting set-back after heating the samples to 140 °C and proportion of other components (lipids  $r = -0.96$ ;  $p = 0.024$ , ash  $r = -0.98$ ;  $p = 0.002$ ). The hull starch was the least pure starch and produced the weakest gels. In the presence of amylose, addition of lipids has been found to reduce paste viscosities because of formation of short pastes [67]. Richardson et al. [63, 68] have also shown that amylose gels with emulsifiers produce weaker gels because the amylose aggregates into clusters, not into networks. For some starches these types of aggregates are only induced after high temperatures, possibly because of the amylose melting [63]. When heating starch to 140 °C, increasing amylose content had a significant effect in increasing the breakdown viscosity ( $r = 0.97$ ;  $p = 0.013$ ). In previous studies [13, 14, 66,] when heating of samples was just to 95 °C, a negative correlation has been observed. A correlation between higher amylose molecular weight (mw) and higher pasting temperature was also observed ( $r = 0.97$ ;

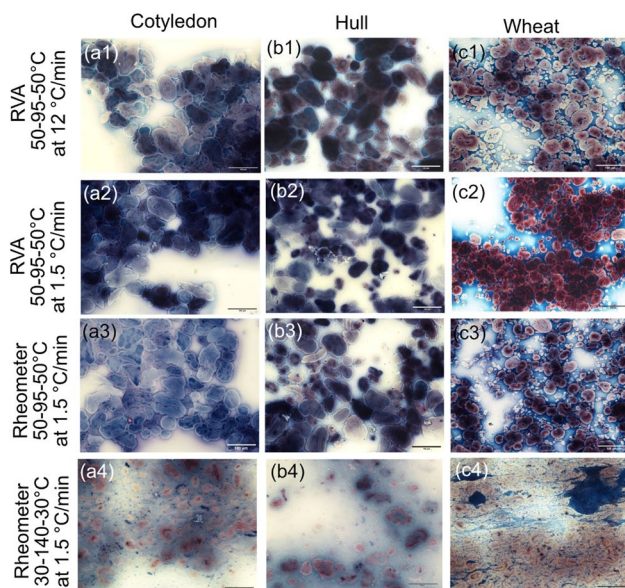


**Fig. 9** Smears of starch pastes at the end of rheological heating cycles. The blue areas are amylose and the pink/brown amylopectin. **a** Faba bean cotyledon starch; **b** faba bean hull starch; **c** wheat starch; **(1)** Rapid viscosity analysis (RVA) heating profile 50–95–50 at heating rate 12 °C/min; **(2)** RVA heating profile 50–95–50 at heating rate 1.5 °C/min; **(3)** rheometer heating profile 50–95–50 at heating rate 1.5 °C/min; **(4)** Rheometer heating cycle 30–140–30 °C at heating rate 1.5 °C/min; Scale bar = 100 μm

$p=0.016$ ) whilst negative correlation was found with amylose molecular weight (mw) and breakdown viscosity after heating the samples to 140 °C ( $r = -0.96$ ;  $p= 0.04$ ). These correlations indicate that larger amylose molecules required more energy to melt and are more difficult to breakdown; however, more research is necessary to validate this theory.

To our knowledge, this is the first time faba bean starch has studied at temperatures up to 140 °C by using rheometry and microscopy. The research results revealed that by altering the heating rate, temperature ranges and instruments, different starch paste textures can be achieved. This research is relevant for many food processes.

## Conclusions

In comparison to wheat, faba bean starch produced more viscous pastes attributed to the larger granules and a higher degree of polymerization. The significantly higher amylose content of the faba bean starch to wheat starch, augmented the gelatinisation temperatures. The cotyledon and hull starch from the same botanical origin were more similar to each other, than to the wheat, however, some differences were noted. Compared with the cotyledon starch, the hull starch displayed higher gelatinisation temperature and lower pasting viscosity, possibly due to a higher lipid and resistant starch content creating short pastes.

For all starches, the apparent viscosity was higher when the heating rate was higher (12 °C/min compared to 1.5 °C/min) because of increased granular swelling. Paste viscosities were higher in the RVA than in the fully sealed rheometer, presumably because of a higher water evaporation during the heating. Peak viscosity and breakdown viscosity were achieved at a high temperature cycle (30–140–30 °C), causing substantial breakdown of the swollen granules, which reduced the final viscosities of the starch gels after cooling.

From the results, it can be speculated that food products containing faba bean starch will gelatinise at higher temperature and be more viscous, both during and after heating, than products with wheat starch. Firmness of the food products can also be tailored by controlling heating rate, type of heating vessel and temperature ranges.

**Supplementary Information** The online version contains supplementary material available at <https://doi.org/10.1007/s11694-022-01543-7>.

**Acknowledgements** The authors gratefully acknowledge Galia Zamaratskaia for reviewing the paper and Astrid Gumucio and Anna-Greta Haglund efforts in protein and fat analysis.

**Author Contributions** “Conceptualization, KN and ML.; methodology, KN and ML.; validation, KN and ML; formal analysis, KN.; investigation, KN, HDÖ, FV and CS ; resources, MHe and ML ;

writing—original draft preparation, KN; writing—review and editing, HDÖ, FV , CS, MH and ML; visualization, KN.; supervision, Corine Sandström. MH and ML.; funding acquisition, ML. All authors commented on previous versions of the manuscript. All authors read and approved the final manuscript.”

**Funding** Open access funding provided by Swedish University of Agricultural Sciences. Svenska Forskningsrådet Formas (2018-018699), Lantmännen Research Foundation (2017F003), and Trees and Crops for the Future (TC4F).

## Declarations

**Conflict of interest** “The authors declare no conflict of interest.” “The funders had no role in the design of the study; in the collection, analyses, or interpretation of data; in the writing of the manuscript, or in the decision to publish the results”.

**Open Access** This article is licensed under a Creative Commons Attribution 4.0 International License, which permits use, sharing, adaptation, distribution and reproduction in any medium or format, as long as you give appropriate credit to the original author(s) and the source, provide a link to the Creative Commons licence, and indicate if changes were made. The images or other third party material in this article are included in the article's Creative Commons licence, unless indicated otherwise in a credit line to the material. If material is not included in the article's Creative Commons licence and your intended use is not permitted by statutory regulation or exceeds the permitted use, you will need to obtain permission directly from the copyright holder. To view a copy of this licence, visit <http://creativecommons.org/licenses/by/4.0/>.

## References

1. R.E.H. Sims, *Energy-Smart Food for People and Climate - Issue Paper* (FAO, Rome, 2011)
2. EAT-Lancet Commission: Summary Report of the EAT-Lancet Commission. (2019)
3. E. Rööös, G. Carlsson, F. FerawatI, M. Hefni, A. Stephan, P. Tidåker, C. Witthöft, Less meat, more legumes: prospects and challenges in the transition toward sustainable diets in Sweden. *Renew. Agric. Food Syst.* **35**, 192–205 (2018)
4. Jordbruksverket; Statistiska centralbyrån; Skörd av spannmål, trindsäd, oljeväxter, potatis och slättervall 2019. SCB (2020)
5. Hellsten, S.A., Hann, S., Johanna, M.E.: Åtgärder och väg framåt för att minska kväve- och fosforanvändningen i samhället. IVL Svenska Miljöinstitut (2019)
6. M. Fouad, N. Mohammed, H. Aladdin, A. Ahmed, Z. Xuxiao, B. Shiyang, Y. Tao, Faba bean, in *Genetic and Genomic Resources of Grain legumes Improvement*. ed. by S. Mohar et al. (Elsevier, Amsterdam, 2013), pp. 113–136
7. M.J. Messina, Legumes and soybeans: overview of their nutritional profiles and health effects. *Am. J. Clin. Nutr.* **70**, 439S–450S (1999)
8. F. Guillon, M.M. Champ, Carbohydrate fractions of legumes: uses in human nutrition and potential for health. *Br J Nutr* **88**(Suppl 3), S293–306 (2002)
9. Y. Ren, T.Z. Yuar, C.M. Chigwedere, Y. Ai, A current review of structure, functional properties and industrial applications of pulse starches for value-added utilization. *Compr. Rev. Food Sci. Food Saf.* **20**, 3061–3092 (2021)

10. I.A. Wani, D.S. Sogi, A.M. Hamdani, A. Gani, N.A. Bhat, A. Shah, Isolation, composition, and physicochemical properties of starch from legumes: a review. *Starch - Stärke* **68**, 834–845 (2016)
11. S. Punia, S.B. Dhull, K.S. Sandhu, M. Kaur, Faba bean (*Vicia faba*) starch: structure, properties, and in vitro digestibility: a review. *Legume Sci.* **1**, e18 (2019)
12. N. Singh, Functional and physicochemical properties of pulse starch, in *Pulse Foods Processing, Quality and Nutraceutical Applications*. ed. by B.K. Tiwari, A. Gowen, B. McKenna (Academic Press, London, 2021), pp. 87–112
13. F.L. Stoddard, Starch chemistry, in *Reference Module in Food Science*. ed. by G. Smithers (Elsevier, Amsterdam, 2016), pp. 1–7
14. P. Ambigaipalan, R. Hoover, E. Donner, S. Liu, Q. Jaiswal, R. Chibbar, K.K.M. Nantanga, K. Seetharama, Structure of faba bean, black bean and pinto bean starches at different levels of granule organization and their physicochemical properties. *Food Res. Int.* **44**, 2962–2974 (2011)
15. Z. Zhang, X. Tian, P. Wang, H. Jiang, W. Li, Compositional, morphological, and physicochemical properties of starches from red adzuki bean, chickpea, faba bean, and baiyue bean grown in China. *Food Sci. Nutr.* **7**, 2485–2494 (2019)
16. L. Li, T.Z. Yuan, R. Setia, R.B. Raja, B. Zhang, Y. Ai, Characteristics of pea, lentil and faba bean starches isolated from air-classified flours in comparison with commercial starches. *Food Chem.* **276**, 599–607 (2019)
17. R. Hoover, T. Hughes, H.J. Chung, Q. Liu, Composition, molecular structure, properties, and modification of pulse starches: a review. *Food Res. Int.* **43**, 399–413 (2010)
18. E. Bertoft, Understanding starch structure: recent progress. *Agronomy* **7**, 56 (2017)
19. M.A. Glaring, C.B. Koch, A. Blennow, Genotype-specific spatial distribution of starch molecules in the starch granule: a combined CLSM and SEM approach. *Biomacromolecules* **7**, 2310–2320 (2006)
20. C. Gernat, S. Radosta, D. Damaschun, Supramolecular structure of legume starches revealed by X-Ray scattering. *Starch/stärke* **42**, 175–178 (1990)
21. Y. Ai, J.-L. Jane, Gelatinization and rheological properties of starch. *Starch - Stärke* **67**, 213–224 (2015)
22. N.U. Haase, H.L. Shi, A characterization of Faba Bean starch (*Vicia faba* L.). *Starch/Stärke* **43**, 205–208 (1991)
23. S. Balet, A. Guelpa, G. Fox, M. Manley, Rapid Visco Analyser (RVA) as a tool for measuring starch-related physicochemical properties in cereals: a review. *Food Anal. Methods* **12**, 2344–2360 (2019)
24. R. Tester, W. Morrison, Swelling and gelatinization of cereal starches. I. Effects of amylopectin, amylose and lipids. *Cereal Chem.* **67**, 551–557 (1990)
25. P. Ambigaipalan, R. Hoover, E. Donner, Q. Liu, Retrogradation characteristics of pulse starches. *Food Res. Int.* **54**, 203–212 (2013)
26. M. Kaur, K.S. Sandhu, S.-T. Lim, Microstructure, physicochemical properties and in vitro digestibility of starches from different Indian lentil (*Lens culinaris*) cultivars. *Carbohydr. Polym.* **79**, 349–355 (2010)
27. A.P. Nugent, Health properties of resistant starch. *Br. Nutr. Found.* **30**, 27–54 (2005)
28. Sverigeförsöken: Sverigeförsöken Trial report 2012 Middle Sweden. (2012)
29. H.J. Lee, *The isolation and characterisation of starches from legume grains and their application in food formulations* (RMIT University, Melbourne, 2007), p. 197
30. AOAC International, *Official Methods of Analysis*, 17th edn. (AOAC International, Rockville, 2000)
31. S.H. Yun, N.K. Matheson, Estimation of amylose content of starches after precipitation of amylopectin by concanavalin-A. *Starch/Starke* **42**, 302–305 (1990)
32. Nordic Committee on Food Analysis, *Nitrogen. Determination in food and feed according to Kjeldahl* (Nordic Committee on Food Analysis, Bergen, 1976), p. 6
33. European Commission: Determination of crude oils and fat. Official Journal of the European Communities, (2009)
34. L. Dunn Jr., W. Krueger, Branching ratios of starch via proton nuclear magnetic resonance and their use in determining amylose/amylopectin content: evidence for three types of amylopectin. *Macromol. Symp.* **140**, 179–186 (1999)
35. M. Gidley, Quantification of the structural features of starch polysaccharides by NMR spectroscopy. *Carbohydr. Res.* **139**, 85–93 (1985)
36. G. Nilsson, K. Bergquist, U. Nilsson, L. Gorton, Determination of the degree of branching in normal and amylopectin type potato starch with <sup>1</sup>H-NMR spectroscopy. Improved resolution and two-dimensional spectroscopy. *Starch/Stärke* **48**, 352–357 (1996)
37. F. Vilaplana, R.G. Gilbert, Two-dimensional size/branch length distributions of a branched polymer. *Macromolecules* **43**, 7321–7329 (2010)
38. H.M. Rietveld, A profile refinement method for nuclear and magnetic structures. *J. Appl. Crystallogr.* **2**, 65–71 (1969)
39. H.D. Özeren, R.T. Olsson, F. Nilsson, M.S. Hedenqvist, Prediction of plasticization in a real biopolymer system (starch) using molecular dynamics simulations. *Mater. Des.* **187**, 108387 (2019)
40. P.H. Hermans, A. Weidinger, Quantitative X-ray investigations on the crystallinity of cellulose fibers. A background analysis. *J. Appl. Phys.* **19**, 491–506 (1948)
41. M. Johansson, D. Johansson, A. Ström, J. Rydén, K. Nilsson, J. Karlsson, R. Moriana, M. Langton, Effect of starch and fibre on faba bean protein gel characteristics. *Food Hydrocolloids* **131**, 107741 (2022)
42. H.N. Englyst, S.M. Kingman, J.H. Cummings, Resistant starch: Measurement in foods and physiological role in man, in *Plant Polymeric Carbohydrates*, vol. 134, ed. by F. Meuser, D.J. Manners, W. Seibel (The Royal Society of Chemistry, Cambridge, 1993), pp. 137–146
43. R. Hoover, Y. Zhou, In vitro and in vivo hydrolysis of legume starches by  $\alpha$ -amylase and resistant starch formation in legumes—a review. *Carbohydr. Polym.* **54**, 401–417 (2003)
44. C. Li, A. Wu, W. Yu, Y. Hu, E. Li, C. Zhang, Q. Liu, Parameterizing starch chain-length distributions for structure-property relations. *Carbohydr. Polym.* **241**, 116390 (2020)
45. R. Bajaj, N. Singh, A. Kaur, N. Inouchi, Structural, morphological, functional and digestibility properties of starches from cereals, tubers and legumes: a comparative study. *J. Food Sci. Technol.* **55**, 3799–3808 (2018)
46. K. Dome, E. Podgorbunskikh, A. Bychkov, O. Lomovsky, Changes in the crystallinity degree of starch having different types of crystal structure after mechanical pretreatment. *Polymers* **12**, 641 (2020)
47. V. Vamadevan, E. Bertoft, Structure-function relationships of starch components. *Starch - Stärke* **67**, 55–68 (2015)
48. S. Pérez, E. Bertoft, The molecular structures of starch components and their contribution to the architecture of starch granules: a comprehensive review. *Starch - Stärke* **62**, 389–420 (2010)
49. W. He, C. Wei, Progress in C-type starches from different plant sources. *Food Hydrocolloids* **73**, 162–175 (2017)
50. S. Hizukuri, X-ray diffractometric studies on starches. *Agric. Biol. Chem.* **25**, 45–49 (1961)
51. M.J. Gidley, S.M. Bociek, Organization in starches. *J. Am. Chem. Soc.* **107**, 7040–7044 (1985)

52. H. Tang, B. Hills, Use of  $^{13}\text{C}$  MAS NMR to study domain structure and dynamics of polysaccharides in the native starch granules. *Biomacromolecules* **4**, 1269–1276 (2003)
53. K. Morgan, R. Furneaux, N. Larsen, Solid-state NMR studies on the structure of starch granules. *Carbohydr. Res.* **276**, 387–399 (1995)
54. F. Zhu, NMR spectroscopy of starch systems. *Food Hydrocolloids* **63**, 611–624 (2017)
55. J. Cai, C. Cai, J. Man, W. Zhou, C. Wei, Structural and functional properties of C-type starches. *Carbohydr. Polym.* **101**, 289–300 (2014)
56. M. Paris, H. Bizot, J. Emery, J.Y. Buzare, A. Buleon, NMR local range investigations in amorphous starchy substrates I. Structural heterogeneity probed by  $^{13}\text{C}$  CP-MAS NMR. *Int. J. Biol. Macromol.* **29**, 127–136 (2001)
57. E.A. Meireles, C.N. Carneiro, R.A. DaMatta, R.I. Samuels, C.P. Silva, Digestion of starch granules from maize, potato and wheat by larvae of the the yellow mealworm, *Tenebrio molitor* and the Mexican bean weevil, *Zabrotes subfasciatus*. *J. Insect. Sci.* **9**, 43 (2009)
58. A. Blennow, M. Hansen, A. Schulz, K. Jorgensen, A.M. Donald, J. Sanderson, The molecular deposition of transgenically modified starch in the starch granule as imaged by functional microscopy. *J. Struct. Biol.* **143**, 229–241 (2003)
59. V. Vamadevan, E. Bertoft, Observations on the impact of amylopectin and amylose structure on the swelling of starch granules. *Food Hydrocolloids* **103**, 105663 (2020)
60. N. Singh, J. Singh, L. Kaur, N. Singh Sodhi, B. Singh Gill, Morphological, thermal and rheological properties of starches from different botanical sources. *Food Chem.* **81**, 219–231 (2003)
61. S. Singh, N. Singh, N. Isono, T. Noda, Relationship of granule size distribution and amylopectin structure with pasting, thermal, and retrogradation properties in wheat starch. *J. Agric. Food Chem.* **58**, 1180–1188 (2010)
62. Y.I. Cornejo-Ramírez, O. Martínez-Cruz, C.L. Del Toro-Sánchez, F.J. Wong-Corral, J. Borboa-Flores, F.J. Cinco-Moroyoqui, The structural characteristics of starches and their functional properties. *CyTA J. Food* **16**, 1003–1017 (2018)
63. G. Richardson, S. Kidman, M. Langton, A.-M. Hermansson, Differences in amylose aggregation and starch gel formation with emulsifiers. *Carbohydr. Polym.* **58**, 7–13 (2004)
64. A. Ahuja, R. Lee, A. Latshaw, P. Foster, Rheology of starch dispersions at high temperatures. *J. Texture Stud.* **51**, 575–584 (2020)
65. M. Schirmer, M. Jekle, T. Becker, Starch gelatinization and its complexity for analysis. *Starch Stärke* **67**, 30–41 (2015)
66. M. Schirmer, A. Höchstätter, M. Jekle, E. Arendt, T. Becker, Physicochemical and morphological characterization of different starches with variable amylose/amylopectin ratio. *Food Hydrocolloids* **32**, 52–63 (2013)
67. Y. Ai, J. Hasjim, J.L. Jane, Effects of lipids on enzymatic hydrolysis and physical properties of starch. *Carbohydr. Polym.* **92**, 120–127 (2013)
68. G. Richardson, Y. Sun, M. Langton, A.-M. Hermansson, Effects of Ca- and Na-lignosulfonate on starch gelatinization and network formation. *Carbohydr. Polym.* **57**, 369–377 (2004)

**Publisher's Note** Springer Nature remains neutral with regard to jurisdictional claims in published maps and institutional affiliations.

## Authors and Affiliations

Klara Nilsson<sup>1</sup>  · Corine Sandström<sup>1</sup> · Hüsamettin Deniz Özeren<sup>2,3</sup>  · Francisco Vilaplana<sup>3</sup>  · Mikael Hedenqvist<sup>2</sup>  · Maud Langton<sup>1</sup> 

Corine Sandström  
corine.sandstrom@slu.se

Hüsamettin Deniz Özeren  
ozeren@kth.se

Francisco Vilaplana  
franvila@kth.se

Mikael Hedenqvist  
mikaelhe@kth.se

Maud Langton  
maud.langton@slu.se

<sup>1</sup> Department of Molecular Sciences, SLU - Swedish University of Agricultural Sciences, Box 7015, 750 07 Uppsala, Sweden

<sup>2</sup> Division of Polymeric Materials, Department of Fibre and Polymer Technology, KTH- Royal Institute of Technology, 10044 Stockholm, Sweden

<sup>3</sup> Division of Glycoscience, Department of Chemistry, KTH- Royal Institute of Technology, 10621 Stockholm, Sweden